We are IntechOpen,
the world's leading publisher of
Open Access books
Built by scientists, for scientists

6,900
Open access books available

185,000
International authors and editors

200M
Downloads

154
Countries delivered to

Our authors are among the

TOP 1%
most cited scientists

12.2%
Contributors from top 500 universities

BOOK CITATION INDEX
CLARIVATE ANALYTICS
INDEXED

WEB OF SCIENCE™

Selection of our books indexed in the Book Citation Index
in Web of Science™ Core Collection (BKCI)

Interested in publishing with us?
Contact book.department@intechopen.com

Numbers displayed above are based on latest data collected.
For more information visit www.intechopen.com

Wetting and Drying of Colloidal Droplets: Physics and Pattern Formation

Ruoyang Chen, Liyuan Zhang, Duyang Zang and
Wei Shen

Additional information is available at the end of the chapter

Abstract

When a colloidal droplet is deposited on a solid substrate at ambient condition, it will experience the processes of wetting and drying spontaneously. These ostensibly simple and ubiquitous processes involve numerous physics: droplet spreading and wetting, three-phase contact line motion, flow fields inside droplets, and mass transportation within droplets during drying. Meanwhile, the continuous evaporation of liquid produces inter- and/or intra-molecular interactions among suspended materials and builds up the internal stress within droplets. After drying, interesting and complex desiccation patterns form in the dried droplets. These desiccation patterns are believed to have wide applications, e.g., medical diagnosis. However, many potential applications are limited by the current understanding of wetting and drying of colloidal droplets. This chapter focuses on the complex physics associated with these processes and the pattern formation in the dried colloidal droplets. Moreover, potential applications of these desiccation patterns and prospective works of wetting and drying of the colloidal droplets are outlined in this chapter.

Keywords: colloidal droplets, wetting dynamics and statics, three-phase contact line motion, flow field, mass transport, desiccation patterns

1. Introduction

The formation of complex patterns during wetting and drying of colloidal droplets is commonly observed phenomenon in our daily life, which is also involved in numerous research and industrial fields, e.g., inkjet printing, spray coating, and medical practice. There are various interesting patterns formed by the dried colloidal droplets, e.g., cracking patterns, crystal patterns, ring-stain

patterns, and uniform-deposition patterns. The morphological difference of these desiccation patterns is mainly attributed to the different physical processes experienced by colloidal droplets during wetting and drying; moreover, it is significantly influenced by the complex systems of colloidal fluids and the complicated interactions between the systems and the substrate. These desiccation patterns have potentials to be convenient and low-cost tools for health diagnosis. Therefore, it is intriguing and important to study the physics associated with wetting and drying of colloid droplets and the formation of desiccation patterns in these droplets. Applications of these patterns in medical diagnosis for human beings and animals and prospective work are also covered in this chapter.

2. Wetting and drying of colloidal droplets: physics

2.1. Wetting dynamics and statics

When a colloidal droplet is placed on an ideal solid substrate (flat, smooth and homogeneous), it is far from the state of equilibrium. The droplet will spread on the substrate to respond to the interaction between the droplet and the substrate, i.e., the cohesion of the droplet and the adhesion of the droplet to the substrate. The spreading behaviour of the droplet is mainly driven by three types of forces: surface tension, gravitational force, and viscous force. These acting forces can be quantitatively characterised by relevant dimensionless numbers. The capillary number (C_a) reflects the relationship between viscosity and surface tension:

$$C_a = \frac{\eta u}{\gamma} \tag{1}$$

where u is the characteristic velocity of the three-phase contact line of the colloidal droplet, η and γ are the dynamic viscosity and surface tension, respectively. When the capillary number is low ($C_a < 10^{-5}$), the drop spreading is dominated by surface tension; while the capillary number is high, the liquid surface tension is negligible compared to the viscosity force. The Bond number (B_o) represents the relationship between surface tension and gravity force as follows:

$$B_o = \frac{\rho g h^2}{\gamma} \tag{2}$$

where ρ and h are the density and height of the droplet, and g is the gravitational constant. A low Bond number ($B_o < 1$) indicates that the surface tension dominates the drop spreading.

After reaching equilibrium, the colloidal droplet stops spreading on the surface and forms a contact angle (θ_{eq}) at the three-phase contact line of the droplet (the drop/substrate/air interface), which can be expressed by the Young equation:

$$\cos \theta_{eq} = \frac{(\gamma_{sv} - \gamma_{sl})}{\gamma_{lv}} \tag{3}$$

where γ_{sv}, γ_{sl}, and γ_{lv} are the surface energies of solid-vapour (liquid vapour), solid-liquid, and liquid-vapour surfaces, respectively. However, from a microscopic view, there is a very thin

precursor film with micro/nanometre length in front of the contact line. The thickness of the precursor film is nearly at a monomolecular level, which has been experimentally observed and qualitatively demonstrated in sessile drops [1]. This could be related to the interactions between spreading forces and surface energies [2]. The molecular precursor film could influence the contact angle of the sessile drop. Additionally, real surfaces are seldom automatically smooth, and the real contact angle has never been experimentally observed. Therefore, the apparent contact angle (θ^*) is used to describe the contact angle of the sessile drop on a real surface. If the apparent contact angle of a water droplet on the surface, e.g., polytetrafluor-oethylene (Teflon), alkyl ketene dimmer (AKD) and polyethylene (PE), is higher than 90°, the surface is defined as a hydrophobic surface (low wettability). By contrast, the surface is regarded as the hydrophilic surface (high wettability) such as glass, when $\theta^* < 90°$.

After reaching the equilibrium, the geometric shape of the sessile drop can be estimated by the capillary length (λ_c):

$$\lambda_c = \sqrt{\frac{\gamma}{\rho g}} \tag{4}$$

If the contact radius (R) of the sessile drop is less than the capillary length, the gravitational force is negligible; the droplet will form a spherical cap shape. Therefore, the height (h), volume (V) and surface area (S) can be calculated as follows:

$$h = R\,tan\left(\frac{\theta^*}{2}\right) \tag{5}$$

$$V = \frac{\pi(2 + cos\,\theta^*)(1 - cos\,\theta^*)^2 R^3}{3\,sin^3\theta^*} = \frac{1}{6}\pi h\left(h^2 + 3R^2\right) \tag{6}$$

$$S = \frac{2\pi R^2}{(1 + cos\,\theta^*)} = \pi\left(h^2 + R^2\right) \tag{7}$$

2.2. The dynamics of the three-phase contact line motion

During drying of a sessile drop of solution, two major modes are proposed for the three-phase contact line motion, namely, constant contact area mode and constant contact angle mode [3]. In the constant contact area mode (**Figure 1(a)**), the three-phase contact line remains pinned and the sessile drop is assumed as a wedge-like shape, while the radius remains constant. In the constant contact angle mode (**Figure 1(b)**), the three-phase contact line recedes in a constant profile evolution as the liquid evaporates, leading to a decrease in the radius of the droplet.

In most cases of the colloidal droplet, these two modes occur successively (**Figure 1(c)**). During the first stage, the perimeter of three-phase contact line ($l = 2\pi r_0$) and the contact area ($A = \pi r_0^2$) of the sessile drop remain constant; whereas, the contact angle decreases gradually, and the three-phase contact line gets pinned. In this stage, the drying surface area (S_d) of the sessile drop is equal to its real surface area, i.e., $S_d = S$. According to Eq. (7), the drying surface area decreases with the apparent contact angle (θ^*), resulting in a slight decrease in the average evaporation rate. When the apparent contact angle reaches a receding contact angle, the
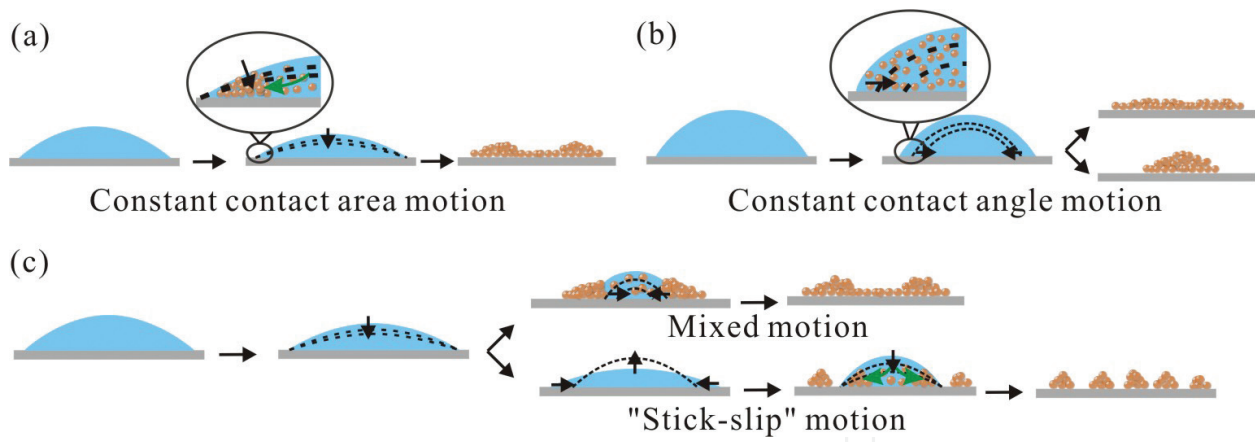
Figure 1. Motion of three-phase contact line in different modes: (a) constant contact area motion; (b) constant contact angle motion; (c) mixed motion and "stick-slip" motion.

second stage starts. In this stage, the evolution of the three-phase contact line is likely to transform to the constant contact angle mode. The three-phase contact line recedes with the propagation of evaporation ($l < 2\pi r_0$), which dominates the decrease in the drying surface area (S_d). As a result, the average evaporation rate of the droplet decreases.

Generally speaking, the local evaporation rate is also determined by the three-phase contact line motion. If the contact line is not pinned during drying, the evaporation rate along the interface of the droplet will be uniform. To the contrary, if the contact line is pinned, the local vapour pressure of the liquid above the droplet is non-uniform; the pressure in the central part is higher than that along the contact line. This makes the local evaporation rate at the contact line greater than that at the central part of the sessile drop.

Interestingly, the drying of colloidal droplets, e.g., the aqueous solution containing silica nanospheres and the ethanol suspension containing titanium dioxide (TiO_2) nanoparticles, sometimes presents a slightly different dynamics of the contact line motion from the typical evolution process [4–6]. During the second stage, if the decreasing contact angle reaches a lower critical value, the contact line will be de-pinned. At the same time, the contact angle and height of the sessile drop will increase, while the base radius will decrease ($r < r_0$). In this case, the contact line tries to get pinned again as the first stage. This motion cycle of de-pinning and re-pinning may successively repeat with further evaporation and is termed as the "stick-slip" motion of three-phase contact line (**Figure 1(c)**). This motion process is more likely to occur in the drying sessile drops of nanofluids and is affected by a number of factors: the wettability of the droplet on the substrate, the thermal conductivity of the substrate, the vapour pressure surrounding the droplet, the environmental temperature, and the relative humidity (RH) [7].

2.3. Flow fields inside the colloidal droplets during drying

Evaporation is a conversion process of volatile solvent from liquid to gas phases. It sponta-neously occurs when the partial vapour pressure in the environment around the sessile drop is lower than the saturation pressure. Natural evaporation of a colloidal droplet is driven by the diffusion of molecules in the volatile solvent. Meanwhile, heat and mass

convections occur within the droplet, building up a local flow field. A number of flow field modes are proposed inside colloidal droplets during their drying. Among these modes, two important flow fields are widely accepted by researchers: the capillary flow and the Marangoni flow.

The capillary flow is a compensation flow, which is induced by the differential evaporation rates along the interface of the droplet during drying [8]. When a colloidal droplet is deposited on an ideal hydrophilic surface, the contact line will be pinned during drying, and the local evaporation rate at the contact line is enhanced, as described in Section 2.2. The enhanced evaporation rate forces the liquid in the central part to flow outwards to replenish the faster liquid loss at the edge, resulting in the horizontally outward capillary flow in the droplet [9]. Within this flow field, the radius of droplet usually remains constant, while the contact angle decreases. The higher evaporation rate of the colloidal droplet leads to a faster decrease in the contact angle. It also causes the three-phase contact line to be pinned faster and the capillary flow within the sessile drop to be stronger. Accordingly, the rate of capillary flow increases along with the increase in evaporation rate of the colloidal droplet during drying [10].

Marangoni flow is a convection flow that is driven by the surface tension gradient in the droplet. This surface tension gradient can be caused by the non-uniform distribution of local temperature field and/or the differential concentration of substances, e.g., suspended particles. For example, during drying of a sessile drop of organic colloidal suspension, e.g., the mica flakes/octane and poly-methyl-methacrylate beads/octane, the liquid evaporation leads to the local variation in the concentration of solid particles and generates a surface tension gradient along the drop-air interface [11, 12]. In this situation, the liquid in the regions with lower surface tension will be pulled towards the regions with higher surface tension, producing the Marangoni convection. The features of the Marangoni flow in a colloidal droplet during drying have been presented by Hu and Larson: the liquid on the surface near the base of the sessile drop is pulled upwards to the top and then is transported downwards, causing the circular movement along the drop-air interface [12]. It is noteworthy that the local surface tension of liquid in the colloidal droplet can be decreased by increasing the local temperature ($\frac{d\gamma}{dT} < 0$), which can cause the temperature-dependent Marangoni flow [3]. This phenomenon is termed as thermo-capillary convection or Bénard-Marangoni convection. The Marangoni flow within a droplet could be described by the dimensionless Marangoni number (M_a) as follows:

$$M_a = -\frac{d\gamma}{dT}\frac{\Delta T L}{\eta \alpha} \tag{8}$$

where ΔT is the temperature difference within the colloidal droplet, L is the characteristic length, η and α are the dynamic viscosity and thermal diffusivity of the droplet, respectively.

The liquid evaporation can cause the hydrodynamic and/or thermodynamic instability within colloidal droplets during drying [13]. This may lead to the simultaneous occurrence of the capillary flow and the Marangoni flow in the droplets [14]. The inward circular Marangoni flow is assumed to counteract the outward capillary flow [9, 14]. Recently, these two flow fields

have been investigated in the water droplets containing polymers on the glass substrate with different controlled temperatures [15]. When the temperature of substrate is lower than the droplet, the Marangoni flow shows stronger than the capillary flow. By contrast, on a heated substrate, the capillary flow is more significant than the Marangoni flow [15].

All of the above flow fields are discussed when the influence of the gravitational force on the droplet can be negligible, i.e., $R \leq \lambda_c$. Nevertheless, when the size of the droplet is much larger than the capillary length ($R \gg \lambda_c$), the gravitational effect should be considered. In this situation, especially for the droplets on heated substrates, another flow field, e.g., Rayleigh-Bénard convection, which is a thermo-gravitational flow, could replace the Bénard-Marangoni convection. For the sessile drop of colloidal suspension on the heated substrate, the temperature gradient induces a concentration gradient of solid particles between the top and the areas close to the three-phase contact line of the droplet [16]. The surface tension of the liquid at the top of the droplet is larger than the one of the areas close to the three-phase contact line, forming the surface tension gradient. Meanwhile, the gravitational force makes the denser liquid transport from the top to the bottom within the droplet. This is called the thermo-gravitational flow, which could be expressed by the Rayleigh number as follows [17]:

$$R_a = \frac{\Delta T \beta g L^3}{\nu \alpha} \tag{9}$$

where β and ν are the thermal expansion coefficient and the kinematic viscosity of the colloidal droplet, in which $\nu = \frac{\eta}{\rho}$. The larger Rayleigh number indicates the more significance of the gravitational effect on the thermo-gravitational flow.

2.4. Mass transportation within the drying droplets

During drying of the colloidal droplet, evaporation-induced local flow filed can give rise to the mass transport. Two ubiquitous phenomena in our daily life are related to the mass transportation within the droplets during drying. They are the "coffee ring" effect and the Marangoni effect. Also, the continuous evaporation of the volatile solvent may cause the aggregation of particles within the sessile drops.

2.4.1. The "coffee ring" effect

When a droplet of coffee is spilt onto a solid substrate, a ring-shaped deposit of coffee solids will be found around the edge of the droplet after completely dried. This phenomenon is called the "coffee ring" effect. The formation of "coffee ring" is a hydrodynamic process attributed to the capillary flow in the droplet during drying, which has been described in Section 2.3. The enhanced evaporation rate at the pinned contact line of the droplet generates the horizontally outward capillary flow; this capillary flow carries the suspended materials, e.g., coffee solids, to the edge. After evaporation, these redistributed materials are concentrated at the edge, thus forming a "coffee ring" at the perimeter of the droplet [8, 9].

There are two essential conditions for the "coffee ring" effect: pinning of the contact line and enhanced evaporation rate at the contact line. If the contact line motion obeys the constant contact angle mode, the suspended materials will be moved inwards by the retraction of the contact line. This process could prevent the ring formation. It is worth mentioning that the pinning of the contact line is dependent on the suspended particles rather than the nature of substrate. The substrate only provides the conditions for temporarily anchoring the contact line; this may trigger the accumulation of suspended particles there. These highly concentrated particles increase the energy barrier for the movement of the contact line, leading to the indefinite pinning and the ring formation at the edge of the droplet [18].

Many strategies are proposed to limit the "coffee ring" effect. Yunker et al. experimentally demonstrated that the control of the particle shape, e.g., ellipsoidal particles, could suppress the outward transport of spherical particles to the contact line of the droplet, ensuring the uniform deposition of particles [19]. Weon and Je studied different movements of polystyrene microspheres with two different sizes (2 and 20 μm in diameter) within the droplet and observed that the small particles have a greater tendency to move outwards to form the ring-shaped deposits, while the large particles initially moved to the edge and then reversed towards the central part of the droplet. They stated that the geometric constraint of the droplet was responsible for the formation of capillary forces on the large particles, which are in the opposite direction as the outward capillary flow, near the contact line, thus repelling the "coffee-ring" effect [20]. These capillary forces were proportional to the size of the suspended particles, while inversely proportional to the contact angle of the droplet [20, 21]. Recently, Eral et al. showed that the application of electrical potential on the sessile drops, containing DNA solution and colloidal particles of various sizes, could suppress the "coffee ring" effect. This is due to the fact that the electrical potential changes the wettability of the droplet on the substrate and prevents the pinning of the contact line, on the one hand, and produces the internal flow fields that counteract the outward capillary flow, on the other hand [22]. Furthermore, control of the Marangoni flow could counteract the capillary flow, reversing the "coffee ring" effect [14]. Therefore, temperature control of the substrate and addition of some organic mixtures were used to promote the Marangoni flow within the droplet to eliminate the ring formation. Soltman and Subramanian studied the profile of the droplet of inject-printed ink on the poly(4-vinylphenol)-coated glass substrate with controlled temperature and disclosed that a decrease in the temperature of substrate could inhibit the "coffee ring" effect [23]. Most recently, the evaporation rate-controlled regime has been revealed to be an effective way to suppress the "coffee ring" effect of a droplet containing nanoparticles [24]. The principle of this process is similar to the common natural phenomenon of the surface skinning of paint and milk, namely, particles accumulate at the interface of liquid and air. When a sessile drop of nanoparticles is drying under a high evaporation rate, the interface of the droplet shrinks much faster than the diffusion of suspended nanoparticles; in this case, the nanoparticles in the vertical evaporation flow can be captured by the shrinking interface, forming an uniform film of aggregated nanoparticles at the interface of the droplet (the film formation will be further discussed in Section 2.4.3). The "coffee ring" effect within the droplet can be prevented by this nanoparticle film, resulting in the uniform deposition of nanoparticles after complete drying [24].

The "coffee ring" effect discussed above is mainly focused on the sessile drop drying on a solid substrate. When it comes to the porous substrates, the situation could be quite different, which requires the consideration of the additional fluid penetration and removal mechanisms. Rui and Brian compared the microstructural morphologies of ink droplets containing polyethylene glycol (PEG) and zirconium dioxide (ZrO_2) nanoparticles drying on the porous substrates with different pore sizes and proposed that the ring formation is dependent on the pore size. The porous substrates play the role in draining the solvent of the droplet by capillary force. Through this mechanism, the pore size may affect the capillary force and thus influences the flow field within the droplet [25]. Most recently, Shen's group investigated the "coffee ring" effect on filter papers [26]. They found that the "coffee ring" may or may not form on filter papers. This is because of the competition between the driving force of the non-uniform evaporation and the retarding forces caused by the chromatographic and filtration effects on the transport of suspended materials in filter papers. For some filter papers, in which the chromatographic and filtration effects are the dominant retarding forces to the materials transportation, the "coffee ring" effect could be totally avoided [26].

The inhibition of the "coffee ring" effect is desirable in many applications. Hence, more significant research efforts are needed to control the "coffee ring" effect in safe, convenient and low-cost ways.

2.4.2. The Marangoni effect

The "tears of wine" is another interesting phenomenon widely observed in our daily life. It is also known as the "wine legs," which is manifested as a tear-like droplets running down along the side of the glass of wine, especially for the wine with high alcohol content. The "tears of wine" is the result of the Marangoni effect.

Wine is a mixture of alcohol and water, with many suspended and dissolved materials. When the wine encounters the glass, capillary force in the meniscus at the contact line between wine, air and glass walls will make the wine easily climb on the glass. During climbing, the alcohol, which has a higher equilibrium vapour pressure than water, suffers a higher evaporation rate. In the meniscus, because of the large relative surface area versus the small droplet volume, the concentration of alcohol decreases dramatically. The fast depletion of alcohol causes the different concentrations between the meniscus and bulk of wine, thus generating the surface tension gradient between these two regions. The higher surface tension in the regions with lower alcohol concentration pulls up more liquid from the regions with higher alcohol concentration (lower surface tension) to form the droplets. Once the gravitational force on the droplets overcomes the capillary force, they will creep down on the side of the glass and back to the bulk of wine. That is the "tears of wine."

2.4.3. Aggregation of particles

Apart from the redistribution of suspended particles driven by the local flow fields, the liquid evaporation also promotes the movement of the particles. As the evaporation propagates, the tiny menisci will be generated between particles at the interface of the droplet.

These menisci build up a negative Laplace pressure between particles, as shown in **Figure 2** [9]. This Laplace pressure (P_{cap}) is regarded as the compressive capillary force, which could be written as:

$$P_{cap} = -\frac{2\gamma^* \cos \theta_{lp}}{r_m} \tag{10}$$

where γ^* is the surface tension of the pure liquid on the drying layer of the sessile drop, θ_{lp} is the contact angle between the pure liquid and the solid particles, and r_m is the radius of the meniscus. The further evaporation will increase the curvature of the liquid menisci and decrease its radius (r_m). According to Eq. (10), the compressive capillary force will increase as the liquid evaporates; this may drain the liquid through the particle mesoscopic clusters and promote the aggregation of the adjacent clusters [27].

Meanwhile, the entropic depletion force always arises between the large particles in the colloidal suspension containing different sizes of particles [28, 29]. During drying of such colloidal droplets, the Laplace pressure forces the large particles to get closer; this may exclude the small particles from the vicinity of the large particles. This continuous local depletion of small particles produces the depletion force between the large particles and then increases in the osmotic pressure between these particles. As a result, the aggregation of these particles is promoted.

All of the evaporation-induced mass behaviours may or may not form a particle film (skin) at the drop-air interface of the colloidal droplet. It is easy to understand from the macroscopic views. If the colloidal droplet dries slowly and uniformly, the diffusion of suspended particles will be sufficient to maintain an essentially uniform particle concentration within the droplet; this does not favour the formation of the particle skin at the interface. By contrast, if the sessile drop dries fast and non-uniformly, the diffusion of suspended particles is limited, which leads to the increasing concentration of suspended particles at the drop-air interface. Once the concentration of these particles reaches to a critical value, a dense particle skin will form at the interface. The formation of particle skin is sometimes referring to the gelation process [30]. The dimensionless Péclet number (P_e) could be used to predict whether the particle film will be formed or not at the interface of the colloidal droplet during drying:
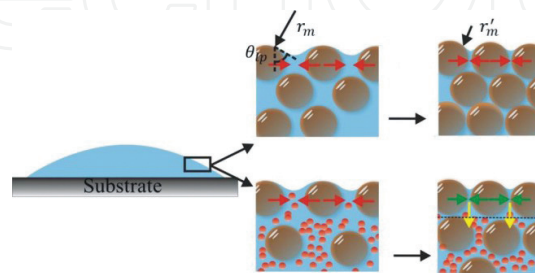
Figure 2. A schematic diagram of the Laplace pressure and the osmotic pressure in a colloidal droplet. The red and green arrows indicate the capillary and depletion forces, respectively. The yellow arrows display the different concentration of the small and red spherical particles.

$$P_e = \frac{Jh_o}{D} \qquad (11)$$

where h_o is the initial height of the sessile drop, D is the diffusion coefficient of the non-volatile particles, and J is the evaporation flux of the sessile drop. The evaporation flux (J) is characterised as the mean flux of the vapour per surface area and is given by Annarelli et al. [31]:

$$J = -\frac{dV}{Sdt} \qquad (12)$$

where S and V are the drying surface area and the volume of the sessile drop at the drying time t, respectively. If $P_e \ll 1$, the particle diffusion will be more significant; this will lead to a homogeneous distribution of the suspended particles within the sessile drop. If $P_e \gg 1$, the diffusion will be too weak to prevent the increase in the particle concentration at the interface, thus producing a dense skin on the surface of the colloidal droplet [32, 33].

3. Wetting and drying of colloidal droplets: pattern formation

Sessile drops of different colloidal suspensions experience different drying processes and evaporation mechanisms. This leads to the formation of various interesting patterns in the dried droplets, which is termed as the desiccation patterns. They are mainly composed of ring-stain patterns, cracking patterns, crystal patterns, and combined patterns [7, 21]. These desiccation patterns are widely observed in the sessile drops of biofluids and nanofluids. In the following sections, the desiccation patterns in these drying sessile drops will be reviewed.

3.1. Sessile drops of biofluids

3.1.1. Sessile drops of blood plasma

Blood plasma is a complicated suspension that behaves like a Newtonian fluid. It mainly contains 90% (by mass) of water, 6% of macromolecular proteins, 1% of inorganic electrolytes, and other minor components [9].

Desiccation patterns are commonly observed in a sessile drop of blood plasma drying on a solid substrate. These patterns are characterised by two distinguished regions: a peripheral region and a central part. Two major patterns generate in these regions. Cracking patterns in orthoradial and radial directions are throughout the whole sessile drop, and crystal patterns with different morphologies accumulate in the central part, as shown in **Figure 3(a)** [9].

The main components of blood plasma can be changed easily by the health condition; this leads to the different desiccation patterns. Meanwhile, these components present different evaporating behaviours and play different roles in the desiccation patterns. Moreover, they may interact with one another during drying. Because of these, it is a challenge to fully understand the underlying mechanisms for the desiccation patterns in the blood plasma.
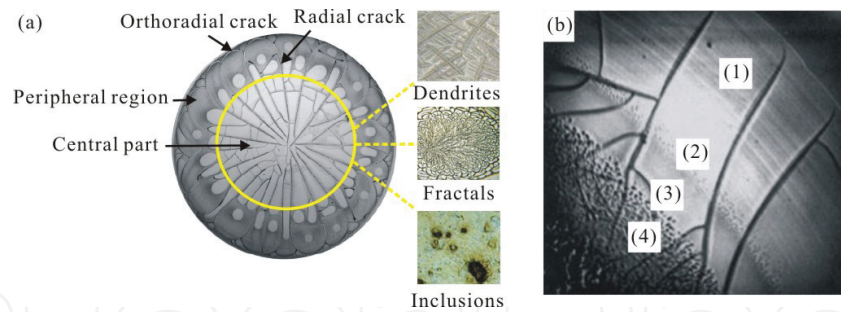
Figure 3. Desiccation patterns in the sessile drop of (a) blood plasma from a healthy adult [9]; (b) morphological details of four regional patterns in the sessile drop of BSA saline solution: (1) homogeneous protein film; (2) protein precipitates, (3) protein gel, and (4) salt crystal [34].

For the sake of better understanding, these desiccation patterns, many simple systems, e.g., bovine serum albumin (BSA) and human serum albumin (HSA) saline solutions (0.9% w/v of NaCl/water), were used to model the complex biofluids. Yakhno conducted a macroscopic study and observed that four distinguished patterns were formed in different regions: homogeneous protein film, protein precipitates, protein gel, and salt crystal, as illustrated in **Figure 3(b)** [34]. In another study, they made the observation on the sessile drop of HSA saline solution and found the similar desiccation patterns as the BSA saline solution [35]. Although these two experiments were carried out by the model macromolecular proteins and saline solution, the desiccation patterns had the similar major feature as the blood plasma: a thick outer ring of aggregated macromolecular proteins with cracking patterns and a flattened central part of accumulated inorganic salts with crystal patterns [3]. Accordingly, these desiccation patterns are referred to plasma patterns.

There are three major factors influencing on the morphologies of these plasma patterns: concentration of inorganic salts, concentration of macromolecular proteins, and the wettability of the droplet on the substrate. Inorganic salts are the main contributors to crystal patterns in the central part [36]. Without inorganic salts, crystal patterns cannot form [37, 38]. Chen and Mohamed investigated the effect of salt concentration on desiccation patterns of the sessile drops of BSA/PBS (phosphate-buffered solution) and observed different crystal patterns in the central part. They suggested that high concentration of salts promoted the aggregation of macromolecular proteins, thus changing the morphologies of crystal patterns [39]. This phenomenon was also observed in the sessile drops of HSA water and saline solutions [37]. According to the Derjaguin-Landau-Verwey-Overbeek theory (DLVO), the stability of a colloidal suspension is dependent on the inter-particle interactions via van der Waal force and Coulombic (electrostatic) force. The van der Waal force is attractive between the particles, while the electrostatic force is repulsive due to the electric double layer of counterions surrounding these particles. The ionic strength of biofluid increases with the increasing salt concentration, leads to the compression of the electric double layer around the macromolecular proteins. This process weakens the repulsive electrostatic force among these proteins, favouring the aggregation of proteins and the subsequent gelation process. Additionally, the diffusion coefficient of macromolecular proteins (D) depends on the ionic strength of colloidal suspension; it decreases proportionally to the increase in the ionic strength [38]. According to

Eq. (11), the lower diffusion coefficient (D) leads to a higher Péclet number (P_e), which means the less effect of the diffusion on the skin formation (gelation) at the interface of the droplet. Therefore, the sessile drop with higher salt concentration is more prone to gelation during drying, forming different desiccation patterns.

Concentrations of macromolecular proteins, e.g., BSA and HSA, are also responsible for the morphologies of desiccation patterns of the dried sessile drop. Tarasevich et al. observed the drying of sessile drops of BSA water and saline solutions with different BSA concentrations and indicated that the BSA concentration influenced on both of the cracking and crystal patterns [38]. The impact of protein concentration on the desiccation patterns was also reported in the sessile drops of HSA water and saline solutions [37, 40]. The effect of protein concentration on the desiccation patterns is related to the gelation because the increase in protein concentration slightly shortens the gelation time of the droplet and increases the initial spacing of radial cracks in the gelled film [31].

Different substrates also result in different morphologies of plasma patterns. Esmonde-White et al. considered that the wettability of the droplet on the substrate played the important role in the apparent contact angle of the sessile drop [41]. This may further influence on the three-phase contact line motion behaviours and the mass transportation during drying. As a consequence, different desiccation patterns form on different substrates.

The drying process of a colloidal droplet is termed as the directional drying because the propagation of evaporation-induced solidification is directed from the edge to the central part. When a droplet of blood plasma is deposited on the solid substrate, the enhanced evaporation rate at the contact line leads to the redistribution of suspended matters. These matters accumulate at the peripheral region and then start to form a film from the edge; this induces the gelation of the droplet. At first, the edge of the sessile drop dries, while the central part remains liquid [42]. In this case, the evaporation-induced shrinkage of the droplet starts from the gelled edge, building up the local stress. However, this shrinkage-caused local stress is constrained by the adhesion of sessile drop to the substrate. The competition between these two stresses results in the tensile stress on the gelled film. Once the tensile stress reaches the level of the local tensile strength, cracking will happen. Typically, the regularly spaced radial cracks occur first and propagate inwards with the retreating of the solidification front. After that, the orthoradial cracks appear parallel to the retreating solidification front [31]. This is the result of the more significance of the orthoradial tensile stress (σ_o) on the gelling film at the edge of the droplet than the radial tensile stress (σ_r), i.e., ($\frac{\sigma_o}{\sigma_r} \gg 1$) [43].

Apart from cracking patterns, crystal patterns in the central part of the droplet have attracted increasing attention of researchers. Some researchers suggested that crystal patterns were composed of the aggregation of macromolecular proteins and the crystallisation of inorganic salts; they further indicated that the increase in inorganic salts promoted the aggregation of proteins [39, 44]. However, Yakhno et al. proposed another explanation to crystal patterns and experimentally demonstrated that these patterns are the salt crystals in the gelled protein matrix; they also argued that proteins only served as seeds for the growth of salt crystals [45, 46]. With current analytical techniques, it is still difficult to clearly distinguish the major

components of these crystal patterns. Therefore, the formation mechanisms of crystal patterns are still not well understood.

3.1.2. Sessile drops of whole blood

Whole human blood is a biological suspension that behaves like a non-Newtonian fluid. It is composed of plasma (55% by volume) and cellular components (45% by volume), i.e., red blood cells (RBCs), white blood cells (WBCs), and platelets; RBCs, WBCs, and platelets represent 97%, 2%, and 1% of the total volume of these cellular components, respectively [9].

Desiccation patterns in the dried sessile drop of whole human blood are significantly different from those of blood plasma without cellular components [47, 48]. Patterns in the blood droplet from healthy adults drying on the glass substrates are comprised of three distinguished zones with different characteristic cracking patterns, as displayed in **Figure 4**. They are, from outer to inner, a fine peripheral region adhering to the substrates, a coronal region with regularly ordered radial cracks and large-sized deposit plaques and a central part with disordered chaotic cracks and small-sized deposit plaques [47].

Desiccation patterns of the blood droplet are strongly affected by the external drying conditions, such as the relative humidity (RH) and the wettability of the blood droplet on the substrates [48–51]. Zeid and Brutin compared the desiccation patterns of blood sessile drop drying under different RHs and found obvious difference between these patterns [50]. The influence of the RH on the desiccation patterns of the blood droplet is related to two main aspects. On the one hand, the initial apparent contact angle of the blood droplet decreases linearly with the increase in RH; this will further influence the dynamic of contact line motion and the evaporation flux of the droplet, as well as the redistribution of suspended particles, e.g., RBCs. As a result, different desiccation patterns form under different RHs. On the other hand, a larger RH can lower the evaporation rate of the blood droplet and prolong its drying time [49]. The liquid remaining under the gelled film can release the evaporation-induced internal stresses, e.g., the capillary pressure and the tensile stress [50]. As mentioned in Section 3.1.1, cracking patterns are originated in the
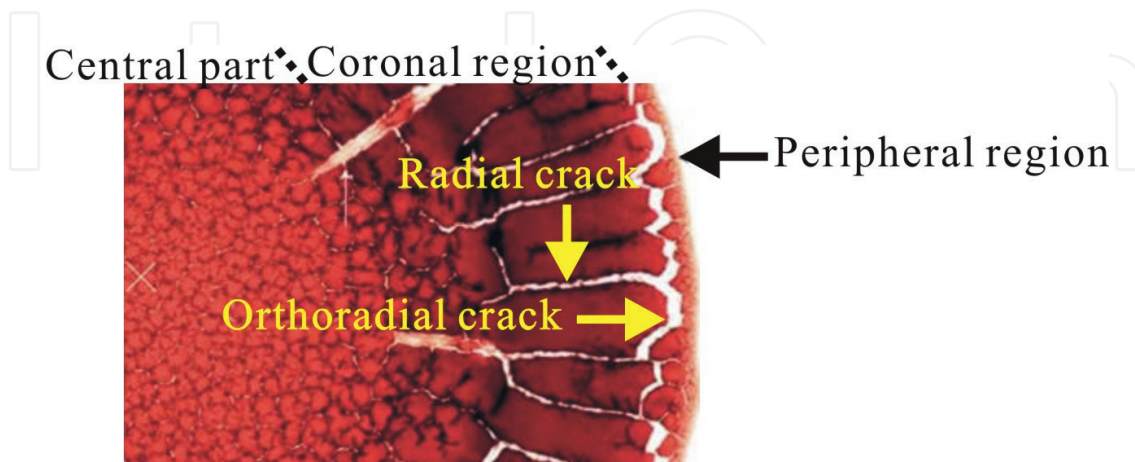

Figure 4. Desiccation patterns of a blood droplet drying on a glass substrate [47].

competition between the shrinkage-induced tensile stress within the gelled film and the adhesion of the droplet to the substrate; as a result, the cracking patterns and the deposit plaques are differing with different RHs.

Brutin et al. studied the desiccation patterns of the blood droplet drying on different substrates and found that desiccation patterns of the droplet on the metallic substrates are dramatically different from those on the glass substrate [48, 51]. The blood droplet on the metallic substrate is nearly hemispherical at the initial stage and, then, forms a uniform glassy skin at the interface; there will be no cracking pattern in the dried droplet. However, the blood droplet on the glass substrate has a lower apparent contact angle at the initial stage and forms a non-uniform solid skin at the interface; after completely dried, it exhibits complex cracking patterns. After comparing the heat and mass transfer within the blood droplet on these substrates, they suggested that the thermal diffusivity of substrates had an insignificant influence on the evaporation dynamics of blood droplet [48]. Subsequently, they attributed these obvious differences of desiccation patterns to the wettability of the blood droplets on these substrates. Because of the different surface energies of these substrates, the apparent contact angle of the blood droplet varies with the substrates. On a hydrophilic glass substrate, the apparent contact angle (θ^*) is close to 20°, while it becomes approximately 90° on the hydrophobic metallic substrates. The evaporation flux at the peripheral region of the blood droplet with low apparent contact angle ($\theta^* < 40°$) is much higher than that in the central part. Nevertheless, the difference in the evaporation flux of the blood droplet with high apparent contact angle ($\theta^* > 90°$) is small [9, 48]. The evaporation behaviours of these blood droplets would therefore be different, leading to the different desiccation patterns.

3.1.3. Sessile drops of other biological fluids

Interesting and complex desiccation patterns are also formed in the sessile drops of other biofluids, e.g., urine, saliva, and tear [52–54]. Yakhno et al. investigated the drying of the sessile drops of urine and saliva from the healthy adults and divided it into three stages: the redistribution of materials leads to the continuous flattening of the droplet; the deposited macromolecular proteins aggregate to form the gel matrix; the inorganic salts induced phase transition of macromolecular proteins to form desiccation patterns [54]. Pearce and Tomlinson investigated desiccation patterns of the tear droplet, as shown in **Figure 5** [55]. They observed a thin amorphous film in the peripheral region, while fern-like patterns in the central part. To study the microstructural morphologies of these desiccation patterns, they employed the scanning electron microscope (SEM) to further observe these regional patterns. The thin amorphous film in the peripheral region presents cracking patterns under the SEM. The fern-like patterns in the central part are composed of dendritic patterns and cubic crystals adjacent to these dendritic patterns. Considering the special components in human tear, e.g., sulphur-containing macromolecular proteins and inorganic salts, they used the energy dispersive X-ray analysis (EDXA) to measure the chemical composition of these patterns and found the present of sulphur-containing macromolecular proteins in the peripheral region. The experimental results also disclosed that dendritic patterns were predominantly made up of sodium and chloride, while cubic crystals were potassium and chloride [55]. López-Solís et al. carried out the further
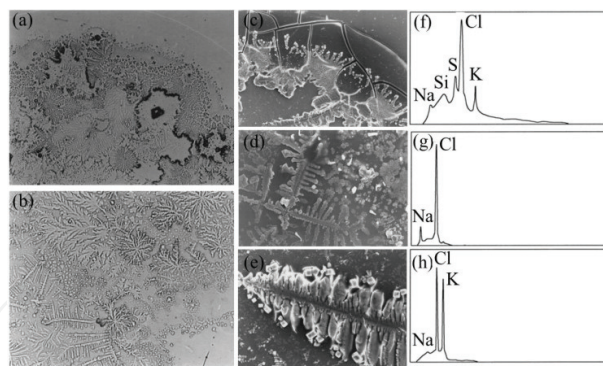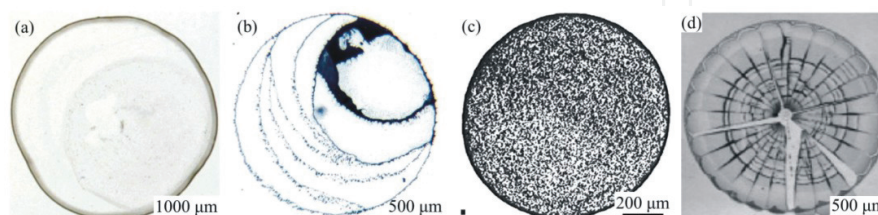
Figure 5. Desiccation patterns in a sessile drop of human tear: (a) thin amorphous film in the peripheral region; (b) fern-like patterns in the central part; (c) cracking patterns in the thin amorphous film; (d) dendritic patterns in the central part; (e) cubic crystals in the central part; (f)–(h) Energy Dispersive X-ray Analysis (EDXA) of the cracked film in (c), dendritic patterns in (d), and cubic crystals in (e), respectively [55].

experiments on desiccation patterns of tear droplets and indicated that the patterns had four distinct zones. They are an outer structured hyaline area with cracking patterns (Zone I), a band of regularly spaced and centripetally oriented crystals (Zone II), a central part comprising randomly distributed fern-like patterns (Zone III) and a circular transition between Zones I and II [52]. The desiccation patterns of tear droplets are quite similar to plasma patterns, including the accumulation of macromolecular proteins at the outer ring and the crystallisation of inorganic salts in the central part.

3.2. Sessile drops of nanofliuds

Nanofluids are the colloidal suspensions of nanoparticles (1–100 nm in size), e.g., metals, oxides, and carbon nanotubes, in a conventional base fluid, e.g., water and ethanol [56]. Various desiccation patterns have been observed in the sessile drops of nanofluids, such as "coffee ring" patterns, multi-ring patterns, uniform-deposition patterns, and cracking patterns, as illustrated in **Figure 6**. Among these patterns, the formation of "coffee ring" patterns is due to the "coffee ring" effect (explained in Section 2.4.1), the multi-ring patterns are related to the "stick-slip" motion of the contact line of the droplet during drying (mentioned in Section 2.3), the uniform-deposition patterns are the result of the inhibition of the "coffee ring" effect caused by the wide

Figure 6. Desiccation patterns of sessile drops of nanofluids: (a) "coffee ring" patterns in the suspension of single-walled carbon nanotube [57]; (b) multi-ring patterns in the suspension of titanium dioxide nanoparticles in ethanol [5]; (c) uniform-deposition patterns in the suspension of graphite nanoparticles [58]; (d) cracking patterns in the suspension of silica nanoparticles [43].

coverage of nanoparticles on the surface of the droplet (referred in Section 2.4.1), and the formation of cracking patterns is connected to the competition between the shrinkage-induced tensile stress and the adhesion of the droplet to the substrates (elaborated in Section 3.1).

These characteristic desiccation patterns can be controlled by different ways. The detailed methods for the inhibition of "coffee ring" patterns have been described in Section 2.4.1. Recently, the transition of desiccation patterns from "coffee ring" patterns to cracking patterns has been found in the droplets of polystyrene nanoparticles as the concentration of nanoparticles increases. This transition is mainly attributed to the uniform distribution of the suspended nanoparticles within the droplet of high concentration of nanoparticles [59]. Most recently, Zang et al. investigated the directional drying of the sessile drops containing polytetrafluoroethylene (PTFE) nanoparticles [13]. The morphological evolution of the sessile drop of PTFE nanoparticles appears to be similar as that of the blood droplet. In the first stage, the gelation starts from the peripheral region, while the central part remains liquid; the wet front recedes as the liquid evaporates, causing the instability in the central part. When it comes to the second stage, the radial cracks occur at the peripheral region and propagate towards the central part. Interestingly, these authors found the surface wrinkling in the gelled zone of the droplet and attributed this phenomenon to the stretching effect caused by the surface tension of liquid in the central part. The surface tension of the hemispheric cap of the liquid in the central part causes the radial stresses on the gelled zone, leading to the flaws in the radial direction. With further liquid evaporation, cracks occur and develop in the radial direction [13]. To inhibit these cracking patterns, these authors added the sodium dodecylsulfate (SDS) into the droplet and suggested that the addition of SDS inhibited the formation of cracking patterns [13]. In another experiment, they studied the drying of the sessile drop containing silica nanoparticles and polyethylene oxide (PEO) additives and indicated that the PEO additives lead to the uniform deposition of silica nanoparticles during drying and to the suppression of cracking patterns after drying [60].

3.3. Applications of desiccation patterns

It is well known that some diseases can cause the changes in the composition of biofluids and the modification in the structure of macromolecular proteins; this may result in the different characteristic desiccation patterns. This implies that desiccation patterns in the sessile drops of biofluid could be used as the simple and low-cost diagnostic tools to identify the health condition of human beings [9].

The medical diagnosis technique based on desiccation patterns of biological droplets has begun with the so-called "Litos" test system in the former Soviet Union three decades ago. This system was developed after it was realised that inorganic salts in the urine droplet of patients with urolithiasis would crystallise to form the distinct desiccation patterns, which enables the diagnosis of urolithiasis at a preclinical stage [61]. After that, the medical diagnosis technique based on desiccation patterns attracted increasing attention of researchers; this is not only because of low-cost but also due to the fact that the diagnosis can be performed by a less-qualified individual [3]. Yakhno et al. presented systematic correlations and analyses of desiccation patterns in the sessile drop of blood serum from healthy individuals and patients
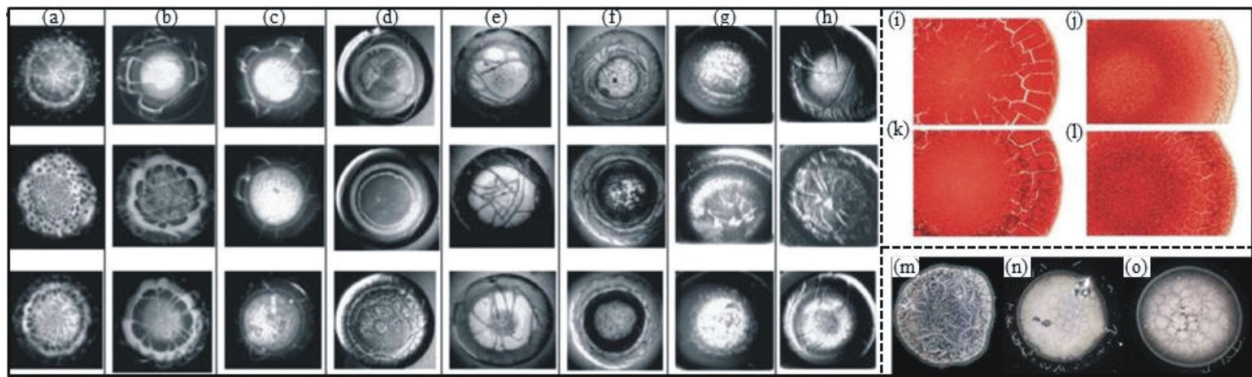
Figure 7. Desiccation patterns of sessile drops of blood serum from (a) healthy individuals and patients with different diseases or physiological states: (b) breast cancer; (c) lung cancer; (d) paraproteinemia; (e) maternal full term delivery; (f) maternal premature delivery; (g) threatened abortion (premature delivery) in different periods of gestation; (h) hepatitis [62]; blood droplets from (i) a 27-year-old healthy female; (j) a patient with anaemia; (k) a 31-year-old healthy male; (l) a patient with hyperlipidaemia [47]; tear droplets from (m) a healthy individual; (n) a 40-year-old female with moderate xerophthalmia; (o) a 72-year-old male with severe xerophthalmia [53].

with different diseases: breast cancer, lung cancer, paraproteinemia, hepatitis, as well as from females with maternal full-term delivery and premature deliveries in different periods, as displayed in **Figure 7(a)–(h)** [62]. They indicated that desiccation patterns in the blood serum droplets from healthy individuals could be easily distinguished with patients suffering from the above-mentioned diseases [62]. Muravlyvova et al. analysed desiccation patterns in the dried plasma droplets from patients with different lung-related diseases from the molecular level and implied that the distinguished patterns in the droplets from patients with interstitial pulmonary disease could be linked to the disease-induced modification of the extracellular nucleic acids and macromolecular proteins [63]. Consequently, the key information locked in desiccation patterns of the blood plasma droplet is believed to be useful for disease diagnosis.

Recently, desiccation patterns in the sessile drops of whole human blood have been reported to be connected to the diagnosis of blood-related diseases, as displayed in **Figure 7(i)–(l)** [47]. **Figure 7(i) and (k)** are the samples from healthy individuals; these two samples exhibit the similar desiccation patterns. **Figure 7(j)** presents the desiccation patterns in the blood droplet from a patient with anaemia. The peripheral region and the outer area of the coronal region are very light in colour and have more plaques compared with the samples from healthy individuals. This could be associated with the deficit of RBCs and low level of haemoglobin in these cells of anaemia sufferers. **Figure 7(l)** illustrates the desiccation patterns in the blood droplet from a patient with hyperlipidaemia. The peripheral region and the outer area of the coronal region are thick and greasy, which is most likely related to the high level of lipoproteins in the blood. Furthermore, the desiccation patterns in the blood droplet from unhealthy people do not have the radial cracking patterns in the coronal region. This could be due to the changed wettability of the blood droplet on the glass substrates caused by the disease-induced modification of blood composition [47].

Desiccation patterns left by the dried tear droplets might also give the indications of the ocular diseases. Traipe-Castro et al. compared the tear droplets from a healthy individual and those from patients with moderate and severe xerophthalmia (dry eyes) and highlighted two different

points between those two samples. The tear droplets from sick people experienced much shorter drying time than that from healthy individual. After drying, the tear droplets from sick people presented the remarkably different patterns with the healthy individual, as indicated in **Figure 7 (m)–(o)** [53]. Although they did not provide the detailed mechanisms of the linkage between the desiccation patterns and the eye diseases, their experimental findings demonstrated that it could be a possible diagnosis for some eye diseases [53].

Most recently, the possible application of desiccation patterns of the biological droplets has been reported in animal detection. Yakhno et al. investigated the desiccation patterns in the sessile drops of milk, serum, and whole blood from the healthy and diseased cows (bovine leukaemia and bovine tuberculosis). They found that the desiccation patterns in the biological droplets from the healthy cows were significantly different from the diseased cows [64].

Although the interpretation of the information locked in desiccation patterns of a sessile drop of biological fluid is believed to be a low-cost and convenient diagnostic tool, there still have some critical questions need to answer. It can be seen from **Figure 7** that desiccation patterns differ from person to person under the similar conditions. Also, desiccation patterns are very sensitive to the drying conditions and the variations in the main composition in the droplets. Therefore, the first question is how to keep the repeatability of these desiccation patterns. In addition, the diagnosis based on desiccation patterns is subjective because it significantly depends on the visual perceptions of researchers. Hence, the second question is how to ensure the objectivity of the analysis on these desiccation patterns.

4. Prospective work

In summary, the physics of three-phase contact line motion, flow fields, and mass transportation play important roles in the wetting and drying of colloidal droplets as well as their pattern formation. Desiccation patterns formed during drying of blood drops find new applications in diagnosis.

Future works are expected to study on the precursor film, e.g., the length, height and main components, the relationship between the three-phase contact line motion and the evaporation flux along the surface of the sessile drop, the underlying mechanisms of evaporation-induced changes of the local flow field, as well as the control of the "coffee ring" effect. Moreover, two critical issues are required to resolve for pattern applications: the repeatability of desiccation patterns and the objectivity of the analysis on these complex patterns.

Acknowledgements

Author details

Ruoyang Chen[1], Liyuan Zhang[1], Duyang Zang[2]* and Wei Shen[1]*

*Address all correspondence to: dyzang@nwpu.edu.cn and wei.shen@monash.edu

1 Department of Chemical Engineering, Monash University, Clayton, Australia

2 Department of Applied Physics, Northwestern Polytechnical University, Xi'an, China

References

[1] Kavehpour H, Ovryn B, McKinley G. Microscopic and macroscopic structure of the precursor layer in spreading viscous drops. Physical Review Letters. 2003;91:196104. DOI: 10.1103/PhysRevLett.91.196104.

[2] Bonn D, Eggers J, Indekeu J, Meunier J, Rolley E. Wetting and spreading. Reviews of Modern Physics. 2009;81:739-805. DOI: 10.1103/RevModPhys.81.739.

[3] Sefiane K. Patterns from drying drops. Advances in Colloid and Interface Science. 2014;206:372-381. DOI:10.1016/j.cis.2013.05.002.

[4] Shanahan M. Simple theory of "stick-slip" wetting hysteresis. Langmuir. 1995;11:1041-1043. DOI: 10.1021/la00003a057.

[5] Moffat J, Sefiane K, Shanahan M. Effect of TiO_2 nanoparticles on contact line stick-slip behavior of volatile drops. The Journal of Physical Chemistry B. 2009;113:8860-8866. DOI: 10.1021/jp902062z.

[6] Adachi E, Dimitrov A, Nagayama K. Stripe patterns formed on a glass surface during droplet evaporation. Langmuir. 1995;11:1057-1060. DOI: 10.1021/la00004a003.

[7] Askounis A, Sefiane K, Koutsos V, Shanahan M. Effect of particle geometry on triple line motion of nano-fluid drops and deposit nano-structuring. Advances in Colloid and Interface Science. 2015;222:44-57. DOI: 10.1016/j.cis.2014.05.003.

[8] Deegan R, Bakajin O, Dupont T, Huber G, Nagel S, Witten T. Capillary flow as the cause of ring stains from dried liquid drops. Nature. 1997;389:827-829. DOI: 10.1038/39827.

[9] Chen R, Zhang L, Zang D, Shen W. Blood drop patterns: formation and applications. Advances in Colloid and Interface Science. 2016;231:1-14. DOI:10.1016/j.cis.2016.01.008.

[10] Kajiya T, Kaneko D, Doi M. Dynamical visualization of "coffee stain phenomenon" in droplets of polymer solution via fluorescent microscopy. Langmuir. 2008;24:12369-12374. DOI: 10.1021/la8017858.

[11] Hu H, Larson R. Analysis of the effects of Marangoni stresses on the microflow in an evaporating sessile droplet. Langmuir. 2005;21:3972-3980. DOI: 10.1021/la0475270.

[12] Hu H, Larson R. Marangoni effect reverses coffee-ring depositions. The Journal of Physical Chemistry B. 2006;110:7090-7094. DOI: 10.1021/jp0609232.

[13] Zhang Y, Qian Y, Liu Z, Li Z, Zang D. Surface wrinkling and cracking dynamics in the drying of colloidal droplets. The European Physical Journal E. 2014;37:1-7. DOI: 10.1140/epje/i2014-14084-3.

[14] Parsa M, Harmand S, Sefiane K, Bigerelle M, Deltombe R. Effect of substrate temperature on pattern formation of nanoparticles from volatile drops. Langmuir. 2015;31:3354-3367. DOI: 10.1021/acs.langmuir.5b00362.

[15] Kim J, Park S, Kim J, Zin W. Polymer transports inside evaporating water droplets at various substrate temperatures. The Journal of Physical Chemistry C. 2011;115:15375-15383. DOI: 10.1021/jp202429p.

[16] Roisman I, Criscione A, Tropea C, Mandal D, Amirfazli A. Dislodging a sessile drop by a high-Reynolds-number shear flow at subfreezing temperatures. Physical Review E. 2015;92:023007. DOI: 10.1103/PhysRevE.92.023007.

[17] Carle F, Brutin D. Convection. In: Brutin D, editor. Droplet Wetting and Evaporation. Oxford: Academic Press; 2015. p. 115-228. DOI: 10.1016/B978-0-12-800722-8.00009-6.

[18] Deegan R. Pattern formation in drying drops. Physical Review E. 2000;61:475-485. DOI: 10.1103/PhysRevE.61.475.

[19] Yunker P, Still T, Lohr M, Yodh A. Suppression of the coffee-ring effect by shape-dependent capillary interactions. Nature. 2011;476:308-311. DOI: 10.1038/nature10344.

[20] Weon B, Je J. Capillary force repels coffee-ring effect. Physical Review E. 2010;82:015305. DOI: 10.1103/PhysRevE.82.015305.

[21] Zhong X, Crivoi A, Duan F. Sessile nanofluid droplet drying. Advances in Colloid and Interface Science. 2015;217:13-30. DOI:10.1016/j.cis.2014.12.003.

[22] Eral H, Augustine D, Duits M, Mugele F. Suppressing the coffee stain effect: how to control colloidal self-assembly in evaporating drops using electrowetting. Soft Matter. 2011;7:4954-4958. DOI: 10.1039/C1SM05183K.

[23] Soltman D, Subramanian V. Inkjet-printed line morphologies and temperature control of the coffee ring effect. Langmuir. 2008;24:2224-2231. DOI: 10.1021/la7026847.

[24] Li Y, Yang Q, Li M, Song Y. Rate-dependent interface capture beyond the coffee-ring effect. Scientific Reports. 2016;6:24628. DOI:10.1038/srep24628.

[25] Dou R, Derby B. Formation of coffee stains on porous surfaces. Langmuir. 2012;28:5331-5338. DOI: 10.1021/la204440w.

[26] Nilghaz A, Zhang L, Shen W. Coffee stains on paper. Chemical Engineering Science. 2015;129:34-41. DOI:10.1016/j.ces.2015.02.017.

[27] Dufresne E, Corwin E, Greenblatt N, Ashmore J, Wang D, Dinsmore A, Cheng J, Xie X, Hutchinson J, Weitzl D. Flow and fracture in drying nanoparticle suspensions. Physical Review Letters. 2003;91:224501. DOI: 10.1103/PhysRevLett.91.224501.

[28] Anachkov S, Danov K, Basheva E, Kralchevsky P, Ananthapadmanabhan K. Determination of the aggregation number and charge of ionic surfactant micelles from the stepwise thinning of foam films. Advances in Colloid and Interface Science. 2012;183–184:55-67. DOI: 10.1016/j.cis.2012.08.003.

[29] Tuinier R, Rieger J, de Kruif C. Depletion-induced phase separation in colloid-polymer mixtures. Advances in Colloid and Interface Science. 2003;103:1-31. DOI: 10.1016/S0001-8686(02)00081-7.

[30] Lu P, Zaccarelli E, Ciulla F, Schofield A, Sciortino F, Weitz D. Gelation of particles with short-range attraction. Nature. 2008;453:499-503. DOI:10.1038/nature06931.

[31] Annarelli C, Fornazero J, Bert J, Colombani J. Crack patterns in drying protein solution drops. The European Physical Journal E. 2001;5:599-603. DOI: 10.1007/s101890170043.

[32] Trueman R, Lago Domingues E, Emmett S, Murray M, Keddie J, Routh A. Autostratification in drying colloidal dispersions: experimental investigations. Langmuir. 2012;28:3420-3428. DOI: 10.1021/la203975b.

[33] Trueman R, Lago Domingues E, Emmett S, Murray M, Routh A. Auto-stratification in drying colloidal dispersions: a diffusive model. Journal of Colloid and Interface Science. 2012;377:207-212. DOI: 10.1016/j.jcis.2012.03.045.

[34] Yakhno T. Salt-induced protein phase transitions in drying drops. Journal of Colloid and Interface Science. 2008;318:225-230. DOI: 10.1016/j.jcis.2007.10.020.

[35] Yakhno T, Kazakov V, Sanin A, Shaposhnikova O, Chernov A. Dynamics of phase transitions in drying drops of human serum protein solutions. Technical Physics. 2007;52:515-520. DOI: 10.1134/S1063784207040196.

[36] Yakhno T, Kazakov V, Sanina O, Sanin A, Yakhno V. Drops of biological fluids drying on a hard substrate: variation of the morphology, weight, temperature, and mechanical properties. Technical Physics. 2010;55:929-935. DOI: 10.1134/S1063784210070030.

[37] Buzoverya M, Shcherbak Y, Shishpor I. Experimental investigation of the serum albumin fascia microstructure. Technical Physics. 2012;57:1270-1276. DOI: 10.1134/S1063784212090071.

[38] Tarasevich Y, Ayupova A. Effect of diffusion on the separation of components in a biological fluid upon wedge-shaped dehydration. Technical Physics. 2003;48:535-540. DOI: 10.1134/1.1576463.

[39] Chen G, Mohamed G. Complex protein patterns formation via salt-induced self-assembly and droplet evaporation. The European Physical Journal E. 2010;33:19-26. DOI: 10.1140/epje/i2010-10649-4

[40] Buzoverya M, Shcherbak Y, Shishpor I, Potekhina Y. Microstructural analysis of biological fluids. Technical Physics. 2012;57:1019-1024. DOI: 10.1134/S1063784212070079.

[41] Esmonde-White K, Esmonde-White F, Morris M, Roessler B. Characterization of biofluids prepared by sessile drop formation. Analyst. 2014;139:2734-2341. DOI: 10.1039/C3AN02175K.

[42] Tarasevich Y, Vodolazskaya I, Bondarenko O. Modeling of spatial-temporal distribution of the components in the drying sessile droplet of biological fluid. Colloids and Surfaces A: Physicochemical and Engineering Aspects. 2013;432:99-103. DOI: 10.1016/j.colsurfa.2013.04.069.

[43] Giorgiutti-Dauphiné F, Pauchard L. Elapsed time for crack formation during drying. The European Physical Journal E. 2014;37:1-7. DOI: 10.1140/epje/i2014-14039-8.

[44] Pauchard L, Parisse F, Allain C. Influence of salt content on crack patterns formed through colloidal suspension desiccation. Physical Review E. 1999;59:3737-3740. DOI:10.1103/PhysRevE.59.3737.

[45] Yakhno T. Complex pattern formation in sessile droplets of protein-salt solutions with low protein content. What substance fabricates these patterns? Physical Chemistry. 2011;1:10-13. DOI: 10.5923/j.pc.20110101.02.

[46] Yakhno T. Sodium chloride crystallization from drying drops of albumin-salt solutions with different albumin concentrations. Technical Physics. 2015;60:1601-1608. DOI: 10.1134/S1063784215110262.

[47] Brutin D, Sobac B, Loquet B, Sampol J. Pattern formation in drying drops of blood. Journal of Fluid Mechanics. 2011;667:85-95. DOI:10.1017/S0022112010005070.

[48] Brutin D, Sobac B, Nicloux C. Influence of substrate nature on the evaporation of a sessile drop of blood. Journal of Heat Transfer. 2012;134:061101. DOI: 10.1115/1.4006033.

[49] Bou-Zeid W, Vicente J, Brutin D. Influence of evaporation rate on cracks' formation of a drying drop of whole blood. Colloids and Surfaces A: Physicochemical and Engineering Aspects. 2013;432:139-146. DOI: 10.1016/j.colsurfa.2013.04.044.

[50] Bou-Zeid W, Brutin D. Influence of relative humidity on spreading, pattern formation and adhesion of a drying drop of whole blood. Colloids and Surfaces A: Physicochemical and Engineering Aspects. 2013;430:1-7. DOI: 10.1016/j.colsurfa.2013.03.019.

[51] Sobac B, Brutin D. Desiccation of a sessile drop of blood: cracks, folds formation and delamination. Colloids and Surfaces A: Physicochemical and Engineering Aspects. 2014;448:34-44. DOI: 10.1016/j.colsurfa.2014.01.076.

[52] López-Solís R, Traipe-Castro L, Salinas-Toro D, Srur M, Toledo-Araya H. Microdesiccates produced from normal human tears display four distinctive morphological components. Biological Research. 2013;46:299-305. DOI: 10.4067/S0716-97602013000300012.

[53] Traipe-Castro L, Salinas-Toro D, López D, Zanolli M, Srur M, Valenzuela F, Cáceres A, Toledo-Araya H, López-Solís R. Dynamics of tear fluid desiccation on a glass surface: a contribution to tear quality assessment. Biological Research. 2014;47:25. DOI: 10.1186/0717-6287-47-25.

[54] Yakhno T, Yakhno V, Sanin A, Sanina O, Pelyushenko A. Protein and salt: spatiotemporal dynamics of events in a drying drop. Technical Physics. 2004;49:1055-1063. DOI: 10.1134/1.1787668.

[55] Pearce E, Tomlinson A. Spatial location studies on the chemical composition of human tear ferns. Ophthalmic and Physiological Optics. 2000;20:306-313. DOI: 10.1046/j.1475-1313.2000.00523.x.

[56] Taylor R, Coulombe S, Otanicar T, Phelan P, Gunawan A, Lv W, Rosengarten G, Prasher R, Tyagi H. Small particles, big impacts: a review of the diverse applications of nanofluids. Journal of Applied Physics. 2013;113:011301. DOI: 10.1063/1.4754271.

[57] Li Q, Zhu Y, Kinloch I, Windle A. Self-organization of carbon nanotubes in evaporating droplets. The Journal of Physical Chemistry B. 2006;110:13926-13930. DOI: 10.1021/jp061554c.

[58] Crivoi A, Duan F. Effect of surfactant on the drying patterns of graphite nanofluid droplets. The Journal of Physical Chemistry B. 2013;117:5932-5938. DOI: 10.1021/jp401751z.

[59] Brutin D. Influence of relative humidity and nano-particle concentration on pattern formation and evaporation rate of pinned drying drops of nanofluids. Colloids and Surfaces A: Physicochemical and Engineering Aspects. 2013;429:112-120. DOI: 10.1016/j.colsurfa.2013.03.012.

[60] Zhang Y, Liu Z, Zang D, Qian Y, Lin K. Pattern transition and sluggish cracking of colloidal droplet deposition with polymer additives. Science China Physics, Mechanics and Astronomy. 2013;56:1712-1718. DOI: 10.1007/s11433-013-5280-5.

[61] Sefiane K. On the formation of regular patterns from drying droplets and their potential use for bio-medical applications. Journal of Bionic Engineering. 2010;7:S82-S93. DOI:10.1016/S1672-6529(09)60221-3.

[62] Yakhno T, Yakhno V, Sanin A, Sanina O, Pelyushenko A, Egorova N, Terentiev I, Smetanina S, Korochkina O, Yashukova E. The informative-capacity phenomenon of drying drops. Engineering in Medicine and Biology Magazine. 2005;24:96-104. DOI: 10.1109/MEMB.2005.1411354.

[63] Muravlyova L, Molotov-Luchanskiy V, Bakirova R, Zakharova Y, Klyuyev D, Bakenova P, Demidchik L, Suleimenova S. Structure-forming properties of blood plasma of patients with interstitial lung diseases. World Journal of Medical Sciences. 2014;10:478-483. DOI: 10.5829/idosi.wjms.2014.10.4.83285.

[64] Yakhno T, Sanin A, Ilyazov R, Vildanova G, Khamzin R, Astascheva N, Markovsky M, Bashirov V, Yakhno V. Drying drop technology as a possible tool for detection leukemia and tuberculosis in cattle. Journal of Biomedical Science and Engineering. 2015;8:1-23. DOI: 10.4236/jbise.2015.81001.